Journal of Computational Physics 229 (2010) 2625–2633

Contents lists available at ScienceDirect

Journal of Computational Physics

journal homepage: www.elsevier.com/locate/jcp

Numerical modeling of transport barrier formation

Mikhail Z. Tokar

Institut für Energieforschung – Plasmaphysik, Forschungszentrum Jülich GmbH, EURATOM-Association, Trilateral Euregio Cluster, D-52425 Jülich, Germany

ARTICLE INFO

Article history:
Received 26 May 2009
Received in revised form 7 December 2009
Accepted 8 December 2009
Available online 15 January 2010

Keywords:
Plasma
Transport equations
Numerical methods

ABSTRACT

In diverse media the characteristics of mass and heat transfer may undergo spontaneous and abrupt changes in time and space. This can lead to the formation of regions with strongly reduced transport, so called transport barriers (TB). The presence of interfaces between regions with qualitatively and quantitatively different transport characteristics impose severe requirements to methods and numerical schemes used by solving of transport equations. In particular the assumptions made in standard methods about the solution behavior by representing its derivatives fail in points where the transport changes abruptly. The situation is complicated further by the fact that neither the formation time nor the positions of interfaces are known a priori. A numerical approach, operating reliably under such conditions, is proposed. It is based on the introduction of a new dependent variable related to the variation after one time step of the original one integrated over the volume. In the vicinity of any grid knot the resulting differential equation is approximated by a second order ordinary differential equation with constant coefficients. Exact analytical solutions of these equations are conjugated between knots by demanding the continuity of the total solution and its first derivative. As an example the heat transfer in media with heat conductivity decreasing abruptly when the temperature *e*-folding length exceeds a critical value is considered. The formation of TB both at a heating power above the critical level and caused with radiation energy losses non-linearly dependent on the temperature is modeled.

1. Introduction

Transport characteristics in diverse media may undergo spontaneous and abrupt changes in time and space. In solid matter this happens by phase transitions [1]. In magnetized fusion plasmas the transport of charged particles and energy across closed magnetic surfaces is often strongly enhanced by diverse micro-instabilities [2]. These instabilities may be, however, spontaneously suppressed, e.g. if the gradients of plasma parameters approach some critical values. As a result regions with strongly reduced transport, so called transport barriers (TB), arise. In fusion devices of tokamak and stellarator types TB exist both at the plasma edge [3] and in the plasma interior [4].

The presence of interfaces between regions with strongly different transport characteristics impose severe requirements to methods and numerical schemes used for solving of transport equations. In approaches based on the discretization of space derivatives, e.g. finite difference, finite volume and finite element methods [5,6], some assumptions are made *a priory* about the behavior of the solution in order to represent derivatives through the solution values in neighboring points. Normally quadratic or higher order splines are adopted. This is, however, doubtful in points where the transport changes abruptly and a significant alteration in the solution gradient takes place. The situation is complicated further by the fact that

E-mail address: m.tokar@fz-juelich.de

0021-9991/$ - see front matter © 2009 Elsevier Inc. All rights reserved.
doi:10.1016/j.jcp.2009.12.009

we do not know in advance both when and where TB will be formatted. Since analytical approaches, see, e.g. Ref. [7], are meaningful for a qualitative analysis of simplified problems only, proper numerical methods have to be developed.

In this paper we present a method which allows to overcome difficulties outlined above. It has been developed on the basis of approaches elaborated previously in Refs. [8,9] but allows to operate with arbitrarily small time steps. This method for numerical integration of parabolic equations for variables dependent on time and one space coordinate has been validated in the framework of activities of the European Task Force on Integrated Tokamak Modeling [10]. It includes two principal steps:

(i) Change over to a new dependent variable related to the variation after one time step of the original variable integrated over the volume; on the contrary to the original variable the new one has the first spatial derivative continuous everywhere, even if the transport characteristics are discontinuous.
(ii) In the vicinity of each grid knot the second order ordinary differential equation (ODE), which governs the new variable, is approximated by ODEs with constant coefficients; exact analytical solutions of these equations are conjugated by requiring the continuity of the total solution and its first spatial derivative; no assumptions on the solution behavior are made by assessing derivatives.

As an example the heat transfer in a medium with heat conductivity decreasing abruptly when the temperature e-folding length exceeds a critical level is considered. First, the situation with a fixed boundary temperature and heating power above the critical level is modeled. It is demonstrated that the final position of the TB interface with the region of high transport depends on the initial conditions and relatively small time steps are needed to reproduce correctly the interface position in the final steady state. Second, the generation of TB under subcritical heating due to radiation losses non-linearly dependent on the temperature is simulated. The found TB phenomenology is reminiscent of observations on tokamak fusion devices.

2. Basic equations

We proceed from a one-dimensional transport equation in a cylindrical geometry for a variable z being a function of time t and the radial coordinate r:

$$\frac{\partial z}{\partial t} = Q - \frac{1}{r}\frac{\partial}{\partial r}(rq) \tag{1}$$

where Q is the density of heat sources and sinks. The heat flux density q has to be provided by a transport model and, in particular, in the case of anomalous transport due to instabilities in hot fusion plasmas [2], it is generally a complex nonlinear function of z, dz/dr, and other parameters. In this paper we assume that q is given by the Fick's law

$$q = -\kappa\, dz/dr \tag{2}$$

where the heat conduction κ is a step-like function of the e-folding length $L_z \equiv -z/(dz/dr)$:

$$\kappa(L_z \geqslant L_z^{cr}) = \kappa_0, \quad \kappa(L_z < L_z^{cr}) = \kappa_1 \ll \kappa_0 \tag{3}$$

with κ_0 and κ_1 being continuous functions of parameters and a prescribed critical value of L_z, L_z^{cr}. For a fixed z the dependence of q on dz/dr with constant κ_0, κ_1 is displayed in Fig. 1. One can see that in the range $q_{\min} \leqslant q \leqslant q_{\max}$ two values of the gradient dz/dr can be realized for the same flux density. This allows formation of an interface between regions with different

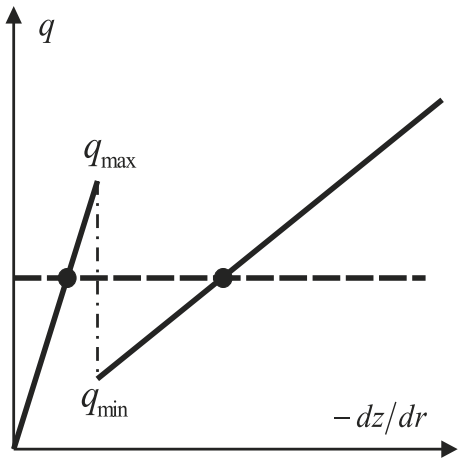

Fig. 1. The dependence of the flux density on the temperature gradient with a step-likely changing heat conduction.

transport: in two neighboring space points with nearly the same z and q the medium can be in states with very differing dz/dr.

In order to go further the partial time derivative is linearly approximated, $\partial z/\partial t \approx (z - z^-)/\tau$, where τ is the time step and $z^-(r)$ the $z(r)$ value at $t - \tau$; higher order Adams–Moulton schemes, see, e.g. [11], can be applied straightforwardly. Differently to the approach in Ref. [9] we operate here by using the variation of the variable z after one time step:

$$\xi = z - z^- \tag{4}$$

This allows to avoid terms becoming arbitrary large by $\tau \to 0$ and, thus, to work with arbitrary small τ. As next we proceed to a volume integrated counterpart to ξ:

$$y = \frac{1}{r^2}\int_0^r \xi\rho d\rho \tag{5}$$

for which the following relationships are valid:

$$\xi = r\frac{dy}{dr} + 2y, \quad \frac{d\xi}{dr} = r\frac{d^2y}{dr^2} + 3\frac{dy}{dr} \tag{6}$$

Since both ξ and y are continuous, the latter has also a continuous first spatial derivative even if the transport characteristics are discontinuous, conversely to the derivatives of z and ξ. By multiplying Eq. (1) by rdr and integrating from 0 to r, one gets the following equation for y:

$$\frac{d^2y}{dr^2} + a\frac{dy}{dr} = by - f \tag{7}$$

where

$$a = \frac{3}{r}, \quad b = \frac{1}{\tau\kappa}, \quad f = \frac{1}{r}\left(\frac{dz^-}{dr} + \frac{1}{r\kappa}\int_0^r Qrdr\right) \tag{8}$$

The advantages of Eq. (7) compared to Eq. (1): (i) there are no derivatives of transport coefficients and, thus, no problems at TB interfaces where $d\kappa/dr$ is infinite and (ii) the flux continuity is taken into account automatically.

Due to symmetry the first space derivative of all variables reduce to zero at the axis, $r = 0$, and from the definition of $d\xi/dr$ we get here $dy/dr = 0$. Therefore theoretically there is no problems with the second term on the left hand side of Eq. (7) with the coefficient a becoming infinite at the axis. Nevertheless, for the numerical realization we transfer the boundary condition from 0 to some finite $r_{\min}$. For this reason we use the Taylor's expansion in the range $0 \leqslant r \leqslant r_{\min}$:

$$y \approx y(r_{\min}) + (r - r_{\min})\frac{dy}{dr}(r_{\min}) + \frac{(r - r_{\min})^2}{2}\frac{d^2y}{dr^2}(r_{\min})$$

where $d^2y/dr^2(r_{\min})$ can be excluded with the help of Eq. (7). This provides

$$\frac{dy}{dr}(0) \approx \frac{dy}{dr}(r_{\min}) - r_{\min}\left[b(r_{\min})y(r_{\min}) - a(r_{\min})\frac{dy}{dr}(r_{\min}) - f(r_{\min})\right]$$

and, by taking into account the definition of a, see Eqs. (8), the boundary condition $dy/dr(0) = 0$ results in:

$$b(r_{\min})y(r_{\min}) - \frac{4}{r_{\min}}\frac{dy}{dr}(r_{\min}) \approx f(r_{\min}) \tag{9}$$

At the outmost border of the calculation domain, $r = r_{\max}$, we assume most generally a boundary condition in the form $uz + vdz/dr = w$. In Section 4 situations with a fixed value of either the solution itself or its e-folding length L_z are considered. In the former case $u = 1,\ v = 0$ and $w = z(r_{\max})$ and in the latter one $u = 1,\ v = L_z(r_{\max})$ and $w = 0$. The boundary condition for the variable y can be obtained by using relations (6) where d^2y/dr^2 is again excluded with the help of Eq. (7). By taking into account the definition of ξ, Eq. (4), one gets

$$\left(2u + \frac{vr}{\tau\kappa}\right)y + ur\frac{dy}{dr} = vrf + w - uz^- - v\frac{dz^-}{dr} \tag{10}$$

3. Approach to numerical solution

The present approach to solve Eq. (7) uses piecewise exact analytical solutions in the vicinity of grid knots. This method differs from those proposed previously, see Refs. [8,9,12], by joining adjacent solutions not in the grid knots but between them. This allows us to avoid in the knots discontinuity of the used approximations to the coefficients a, b and the free term f, and, therefore, to guarantee the continuity of the solution, its first and second derivatives. Consider vicinities $r_i^- \leqslant r \leqslant r_i^+$, where $r_i^\pm = (r_i + r_{i\pm1})/2$, of the grid knots $r_{i=1,\ldots,n}$, with $r_1 = r_{\min}$ and $r_n = r_{\max}$. Here a, b and f are approximated by their values

in the knots, a_i, b_i and f_i, respectively. Thus in any interval $r_i^- \leqslant r \leqslant r_i^+$ Eq. (7) is approximated by a linear second order inhomogeneous ODE with constant coefficients. Its general solution is given by:

$$y^i(r) \equiv y(r_i^- \leqslant r \leqslant r_i^+) = C_{i,1}y_{i,1}(r) + C_{i,2}y_{i,2}(r) + f_i/b_i \tag{11}$$

where the independent solutions of the homogeneous equation, $y_{i,k=1,2}$, are determined by the discriminant $\Delta = a_i^2/4 + b_i$. For a and b from Eqs.(8) Δ is always positive and:

$$y_{i,k} = \exp[\lambda_{i,k}(r - r_i)] \tag{12}$$

where

$$\lambda_{i,k} = -\frac{a_i}{2} - (-1)^k\sqrt{\Delta}$$

For the solution values in the grid knots, $y_i \equiv y(r_i)$, one has

$$y_i = C_{i,1} + C_{i,2} + f_i/b_i \tag{13}$$

At the interfaces of the knot vicinities, $r = r_i^{\pm}$, we require the continuity of the solution and its first derivative. Thus, the following relationships are valid for $2 \leqslant i \leqslant n-1$:

$$\begin{aligned}
&C_{i-1,1}y_{i-1,1,2} + C_{i-1,2}y_{i-1,2,2} + y^0_{i-1} = C_{i,1}y_{i,1,1} + C_{i,2}y_{i,2,1} + y^0_i\\
&C_{i-1,1}y_{i-1,1,2}\lambda_{i-1,1} + C_{i-1,2}y_{i-1,2,2}\lambda_{i-1,2} = C_{i,1}y_{i,1,1}\lambda_{i,1} + C_{i,2}y_{i,2,1}\lambda_{i,2}\\
&C_{i+1,1}y_{i+1,1,1} + C_{i+1,2}y_{i+1,2,1} + y^0_{i+1} = C_{i,1}y_{i,1,2} + C_{i,2}y_{i,2,2} + y^0_i\\
&C_{i+1,1}y_{i+1,1,1}\lambda_{i+1,1} + C_{i+1,2}y_{i+1,2,1}\lambda_{i+1,2} = C_{i,1}y_{i,1,2}\lambda_{i,1} + C_{i,2}y_{i,2,2}\lambda_{i,2}
\end{aligned}$$

where $y_{i,k,m} = y_{i,k}\left(\frac{r_i+r_j}{2}\right)$ with $m = 1,2$ and $j = i + (-1)^m$.

These relations and Eq. (13) applied in the knots i and $i \pm 1$ allow to exclude the coefficients $C_{i,1}$, $C_{i,2}$, $C_{i\pm1,1}$ and $C_{i\pm1,2}$ and, after some cumbersome algebra, we get a recurrent relation between the solution values in neighboring grid points:

$$y_i = y_{i-1}g_{i,1} + y_{i+1}g_{i,2} + \chi_i \tag{14}$$

where

$$\begin{aligned}
g_{i,m=1,2} &= \frac{y_{j,l,l}}{y_{i,l,m}}\left(\tilde{\eta}_{m,l} - \frac{y_{i,l,3-m}}{y_{i,m,l}}\tilde{\eta}_{l,l}\right)\\
\chi_i &= \sum_{m=1,2}\left[\mu_l\left(\frac{y_{i,m,m}}{y_{i,l,m}}\tilde{\eta}_{m,m} - \tilde{\eta}_{l,m}\right) - \frac{f_j}{b_j}g_{i,m}\right]
\end{aligned}$$

with $l = 3 - m$, $\tilde{\eta}_{k,m} = \frac{\eta_{k,m}}{\eta_{1,2}\eta_{2,1} - \eta_{1,1}\eta_{2,2}y_{i,1,1}y_{i,2,2}/y_{i,2,1}/y_{i,1,2}}$,

$$\eta_{k,m} = -(-1)^m\frac{\lambda_{j,m} - \lambda_{i,k} - [\lambda_{j,l} - \lambda_{i,k}]y_{j,l,l}/y_{j,m,l}}{\lambda_{j,1} - \lambda_{j,2}}$$

and

$$\mu_m = -(-1)^m\frac{f_i/b_i - f_j/b_j}{y_{i,l,m}}\frac{\lambda_{j,m} - \lambda_{j,l}y_{j,l,l}/y_{j,m,l}}{\lambda_{j,1} - \lambda_{j,2}}.$$

Relationships (14) and boundary conditions (9) and (10) can be used to find the solution values in all grid knots, $y_{i=1,\ldots,n}$. It is done in the same manner as in standard finite difference, finite volume or finite element methods, see, e.g. Ref. [6]. We briefly review this procedure for completeness of our study. One guesses that there is a linear recurrent relationship

$$y_{i-1} = \delta_i + \varsigma_i y_i \tag{15}$$

By substituting this into Eq. (14), we find the recurrent relations for the parameters δ and ς:

$$\delta_{i+1} = (g_{i,1}\delta_i + \chi_i)/(1 - g_{i,1}\varsigma_i), \quad \varsigma_{i+1} = g_{i,2}/(1 - g_{i,1}\varsigma_i)$$

In order to start the recursion, δ_1 and ς_1 are determined from the boundary condition (9) where $dy/dr(r_{\min}) \approx (y_2 - y_1)/(r_2 - r_1)$ is assumed. An error due to this estimate can be made arbitrary small by decreasing the grid step $h_1 = r_2 - r_1$. With all $\delta_{1,\ldots,n}$ and $\varsigma_{1,\ldots,n}$ found, y_{n-1} and y_n are determined from the relations:

$$y_{n-1} = \delta_n + \varsigma_n y_n, \quad y_{n-1} = \phi + \psi y_n$$

where the parameters ϕ and ψ are obtained from the boundary condition (10) with $dy/dr(r_{\max}) \approx (y_n - y_{n-1})/(r_n - r_{n-1})$. Finally, all y_i are calculated by applying relation (15).

The main difference between the present approach and standard methods mentioned above is the way how the coefficients g and χ are obtained. For example, a linear behavior of the solution between grid points is assumed in finite volume

methods (FVM). In the present approach no assumptions are made and the exact analytical solutions are used. This difference is insignificant for equations with coefficients being smooth functions of r but is of very importance for those with step-like coefficients. In such a case it is also essential to use exact relationships for the derivative of the variable y needed to return to the original quantities ξ and z:

$$\frac{dy}{dr}(r_i) = \sum_{m=1}^{2}\left[\left(y_j - \frac{f_j}{b_j}\right)\frac{y_{j,l,l}}{y_{i,l,m}}\left(\tilde{\eta}_{k,l}\lambda_{i,l} - \frac{y_{i,l,l}}{y_{i,m,l}}\tilde{\eta}_{l,l}\lambda_{i,m}\right) + \lambda_{i,m}\left(\mu_m\frac{y_{i,l,l}}{y_{i,m,l}}\tilde{\eta}_{l,l} - \mu_l\tilde{\eta}_{l,m}\right)\right]$$

One has also to see the principal difference to approaches using other standard discretization techniques, e.g. by applying splines with exponential basis functions. In the present method the basis is defined individually in the vicinity of each grid knot and includes only two functions which are not arbitrary chosen but predetermined by the equation itself. In the case in question of diffusion like equations these solutions have an exponential form (12). The present method can be, however, straightforwardly generalized, see Ref. [8], for equations with negative discriminant Δ whose independent solutions are products of exponential and trigonometric functions.

For non-linear transport problems, like those considered below, a converged solution Z has to be obtained for any time t. This is done in an iterative procedure:

$$Z_{j+1}(r) = Z_j(r)\times(1 - A_{mix}) + z(r)\times A_{mix}$$

Here $Z_j(r)$ is the approximation to the solution after j iterations with $Z_1(r)$ assumed equal to the converged solution at the pervious time moment $t-\tau$, $z(r)$ is calculated with $y(r)$ found by solving Eq. (7) with a, b and f calculated by using $Z_j(r)$. The mixing coefficient $A_{mix}\leqslant 1$ is chosen to minimize the number of iterations needed for convergence. The latter is achieved if the error

$$E = \sqrt{\sum_{i=1}^{n}[z(r_i) - Z_j(r_i)]^2 \Big/ \sum_{i=1}^{n}[z(r_i) + Z_j(r_i)]^2}$$

is reduced to a small fraction of A_{mix} assumed equal to 10^{-5} in the present study.

4. Modeling of transport barrier formation

4.1. Barrier by supercritical heating

Assume a heat source density Q constant over the whole radius and prescribe the value $z(r_{\max})$ as the boundary condition. In a steady state where $\partial z/\partial t = 0$ one gets $q = -\kappa dz/dr = Qr/2$. Thus $L_z = \infty$ at $r = 0$ and in some region near the axis the medium is always in the state of strong transport with $\kappa = \kappa_0$. L_z decreases by approaching to the boundary due to the decrease of both z and $dz/dr < 0$, and at some position a transition to the low transport state with $\kappa = \kappa_1$ is possible. By assuming that this happens at $r = r_*$, one can find the corresponding stationary profile of the dimensionless variable $\Theta = z\kappa_0/(Qr_{\max}^2)$ [9]:

$$\Theta(0\leqslant\rho\leqslant\rho_*) = \Theta(\rho_*) + (\rho_*^2 - \rho^2)/4$$
$$\Theta(\rho_*\leqslant\rho\leqslant 1) = \Theta(\rho_*) + (\rho_*^2 - \rho^2)/(4\chi)$$

where $\rho = r/r_{\max}$, $\rho_* = r_*/r_{\max}$, $\Theta(\rho_*) = (1-\rho_*^2)/(4\chi) + \Theta_1$ with $\chi = \kappa_1/\kappa_0$ and $\Theta_1 = z(r_{\max})\kappa_0/(Qr_{\max}^2)$. For the existence of TB the heat flux density at the interface between regions of high and low transport has to be in the range:

$$q_{\min} \equiv \kappa_1 z(r_*)/L_z^{cr} \leqslant q(r_*) = Qr_*/2 \leqslant q_{\max} \equiv \kappa_0 z(r_*)/L_z^{cr}$$

By taking into account that $z(r_*) = \Theta(\rho_*)Qr_{\max}^2/\kappa_0$, this conditions can be rewritten in the form:

$$\chi\Theta(\rho_*) \leqslant \rho_*/(2\xi) \leqslant \Theta(\rho_*)$$

where $\xi = r_{\max}/L_z^{cr}$. With the requirement $0\leqslant\rho_*\leqslant 1$ these inequalities define the interval of possible ρ_*:

$$\rho_*^{\min} \equiv \sqrt{1/\xi^2 + 1 + 4\chi\Theta_1} - 1/\xi \leqslant \rho_* \leqslant \rho_*^{\max} \equiv \sqrt{\chi^2/\xi^2 + 1 + 4\chi\Theta_1} - \chi/\xi$$

The condition $\rho_*^{\min}\leqslant 1$ guarantees that the interface is located inside the medium and defines the minimum level of the heating power density necessary for the existence of TB, $Q \geqslant 2\kappa_1 z(r_{\max})/(r_{\max}L_T^{cr})$. The latter can be written as a constraint on Θ_1: $\Theta_1 \leqslant (2\chi\xi)^{-1}$.

The analytical consideration above does not make it possible to find the steady state position ρ_* of the interface between regions with different transport characteristics. In order to reveal factors determining ρ_*, Eq. (1) has been solved numerically by the method presented above with the initial condition $\Theta(0,\rho) = \Theta_1 + \alpha(1-\rho^2)/(4\chi)$. By increasing the factor α, we progress from flat initial profiles with low total thermal energy towards peaked ones with higher energy content. Fig. 2 demonstrates stationary profiles found numerically at $t_\infty = 10r_{\max}^2/\kappa_0$ with $\tau = 10^{-3}t_\infty$, on an equidistant spatial grid with $n = 501$, for the parameters $\chi = 0.1$, $\xi = 1$ and $\Theta_1 = 0.01$ ensuring the existence of TB in the final steady state. Analytical

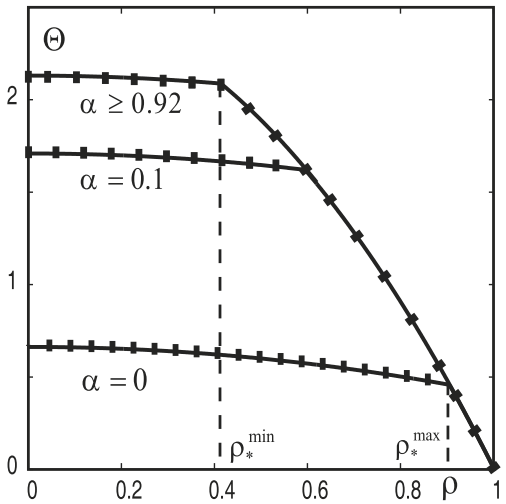

Fig. 2. Final steady state temperature profiles calculated numerically (solid lines) for different initial conditions and found analytically (thick bars) with the positions of the TB interface, ρ_*, determined from the numerical solutions.

solutions with the TB interfaces located at the same ρ_* as those predicted by numerical solutions are shown by thick bars. One can see good agreement between analytical and numerical results and that the whole range $\rho_*^{\min} \leqslant \rho_* \leqslant \rho_*^{\max}$ is realized by changing the initial condition. For $\alpha \geqslant 0.92$ the final state with the broadest TB, i.e., $\rho_* = \rho_*^{\min}$, is realized only. Converged solutions at any time step have been obtained with $A_{mix} = 1$ after 1–2 iterations.

Even if the initial conditions are fixed, different final profiles can be obtained due to deficits in the numerical realization. Fig. 3 displays the Θ-profiles in final stationary states found with the same flat initial temperature profiles, $\Theta(0,\rho) = \Theta_1$, for χ, ξ and Θ_1 as above but with different time steps τ. One can see that the profiles coincide with that shown for $\alpha = 0$ in Fig. 2 only if τ is below a certain value. For larger time steps the solver passes by the correct solution and provides a final state with a too broad TB. This example shows that the possibility to calculate with arbitrary small time step is an important advantage

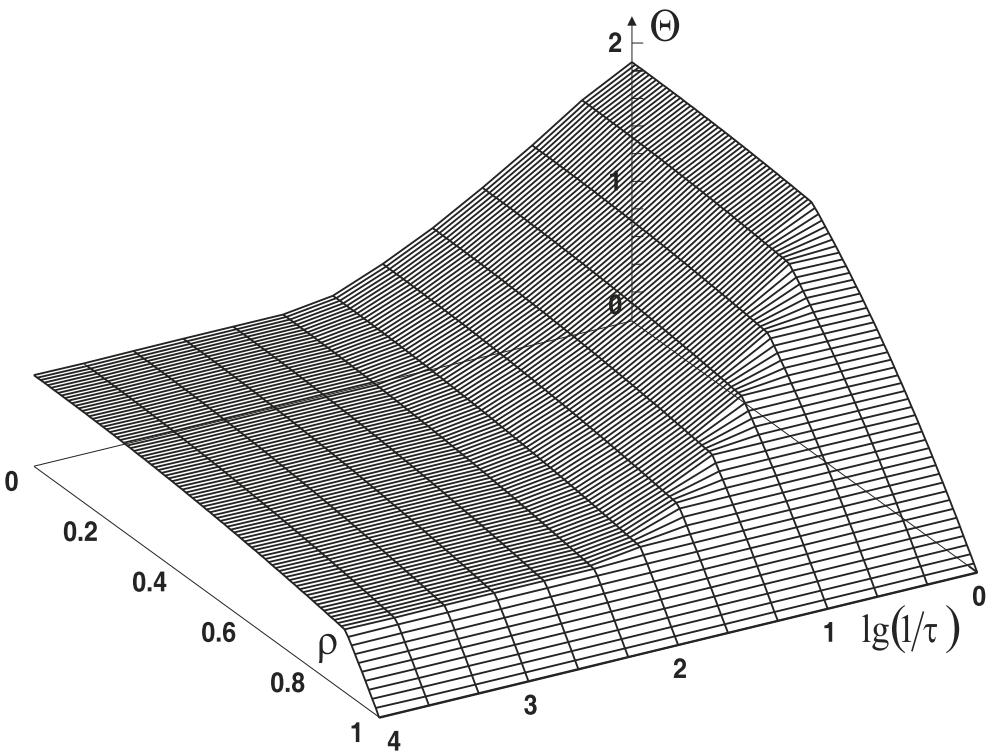

Fig. 3. Final steady state temperature profiles computed with different time steps τ.

of the present approach operating with the alteration of the solution during the time step but not with the solution itself as it has been done before [8,9]. One may say that calculations with a small time step is not a problem for standard approaches, e.g. finite volume method (FVM) [6]. This is, nevertheless, not the case in the situation in question with discontinuous transport characteristics allowing spontaneous formation of transport barriers: calculations with a standard FVM did not provide converged solutions for any A_{mix}.

By concluding this section we compare the results above with those obtained by the method described in Ref. [13], which has been also applied to non-linear transport models allowing bifurcations like the formation of TB. Independently of initial conditions and time step this method provides final stationary state with the TB interface at $\rho_* = \rho_*^{\max}$. In Ref. [13] the solution is found by going from the outmost boundary, $\rho = 1$. If in the point r_{i-1} two solutions are possible, see Fig. 1, the one closest to that in r_i has been selected. This constraint is, probably, too restrictive since it allows transitions between different transport regimes only at $q = q_{\min}$ and $q = q_{\max}$.

4.2. Generation of transport barriers by radiation energy losses

One of paradoxical phenomena in media with non-linear transport properties is the transition to states with reduced transport triggered by additional energy losses dependent in a complex way on the media properties. An example of such a behavior is the formation of a region with reduced heat transport at the plasma edge in tokamak devices by a deliberate seeding of impurities [14]. The suppression of turbulence with increasing electric charge of impurity ions was discussed previously as a possible mechanism of this phenomenon [14].

Here we persevere with the heat conduction law given by Eq. (3) but take into account the radiation energy losses due to excitation of impurity ions by plasma electrons. The volumetric density R of these losses depends in a complex way on the electron temperature z. Roughly [14]:

$$R = R_0 \exp\left[-\left(\sqrt{\frac{z_1}{z}} - \sqrt{\frac{z}{z_2}}\right)^2\right] \tag{16}$$

Here R_0 is proportional to the density of impurity; for temperatures lower than z_1 of several electronvolts only few electrons have enough energy to excite impurity particles; in the range $z_1 \leqslant z \leqslant z_2$ the latter are in "radiant" charge states which can be easily excited; however, impurity ions are too strongly stripped and can not produce intensive radiation if $z > z_2$. For often used neon impurity $z_2 \approx 50$—100 eV and, since a typical temperature in the plasma core is of several keV, the radiation losses are localized at the very plasma edge.

Begin with the case without radiation and a heating power smaller than the critical one for the TB formation, so that $\kappa = \kappa_0$ in the whole plasma. With increasing impurity density and radiation losses the temperature at the plasma edge reduces. At the same time the temperature gradient at the boundary between the core and peripheral layer, where radiation is mainly localized, is maintained roughly the same since the heat flux density towards the edge is fixed by heating power. Therefore with increasing R_0 one can expect an increase of L_z at this boundary and the formation of TB. This intuitive anticipation is confirmed by the results of numerical solution of Eq. (1) where Q has been replaced by $Q - R$ with constant Q and R given by Eq. (16) where $z_1 = 0.01Qr_{\max}^2/\kappa_0$ and $z_2 = 0.03Qr_{\max}^2/\kappa_0$ were assumed. We fix $L_z = 1.01L_z^{cr}$ as the boundary condition at $r = r_{\max}$ to ensure that there is no TB without impurity radiation. As the initial condition the z-profile in the steady state with $R_0 = 0$ has been chosen. Fig. 4(a) shows the final stationary profiles $\Theta(\rho)$ computed for different ratio $\mu = R_0/Q$

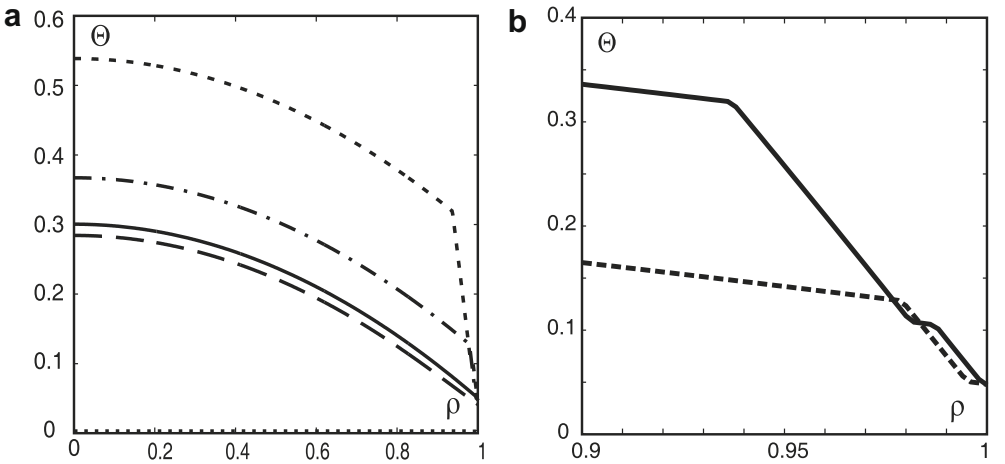

Fig. 4. Final steady state temperature profiles computed for different levels of radiation losses: (a) $\mu = 0$ (solid curve), $\mu = 2$ (long dashed curve), $\mu = 3$ (dash-dotted curve), $\mu = 7$ (short dashed curve) and $\mu = 8$ (dotted curve); (b) detail structure of TB for $\mu = 3$ (dashed curve) and $\mu = 7$ (solid curve).

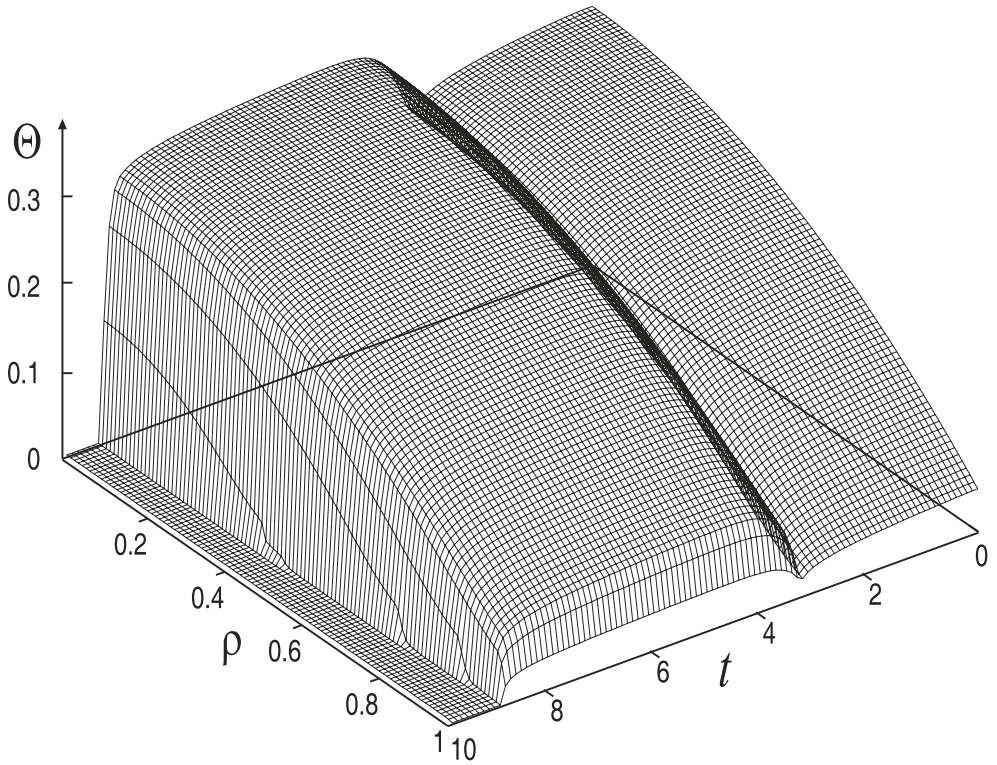

Fig. 5. Time evolution of the temperature profile computed with μ linearly increasing in time, $\mu = 10t/t_\infty$.

with $\chi = 0.1$ and $\xi = 10$. If μ is small enough radiation losses lead to trivial reduction of the temperature everywhere. However, TB arises at the plasma edge if μ is increased up to 3. It becomes even broader if μ is risen further to 7. In this case roughly 200–250 iterations with $A_{mix} = 0.1$ were necessary to get converged solutions with $n = 501$ and $\tau = 10^{-3}$.

For $\mu > 7$ the TB starts to narrow and thermal collapse happens at $\mu = 8$: in the whole plasma the temperature drops to a very low level with $\Theta \equiv 0.0032$ for $0 \leqslant \rho \leqslant 0.86$. This value corresponds to the smallest one of two temperatures at which the exact local heat balance $Q = R$ is satisfied. This state is stable with respect to thermal instability [14]: any small increase (decrease) of the temperature leads to increase (decrease) of radiation losses and fluctuations are suppressed. The second stationary state with $Q = R$ corresponds to $z \approx 0.094$ and is thermally unstable.

In Fig. 4(b) stationary $\Theta(\rho)$-profiles for $\mu = 3$ and 7 are shown in the edge region, $0.9 \leqslant \rho \leqslant 1$. For $\mu = 3$ the temperature profile corresponds well to an intuitively expected one: there is a region attached to the boundary $\rho = 1$ where the temperature gradient and heat transport with conduction are strongly reduced by radiation losses. The temperature gradient increases by moving deeper into the plasma and, because of the decreased temperature, L_z is decreasing below its critical level and a region of reduced transport is formatted. For $\mu = 7$ the temperature profile shape is more complex and a double TB structure exists.

Finally, in Fig. 5 we demonstrate the time evolution of the temperature profile in the case of μ linearly increasing in time, $\mu = 10t/t_\infty$. One can see that TB arises also in this case, however, it does not grow up to the same level as in the previous example with an instantaneous increase of μ because a double TB does not develop.

5. Conclusion

A numerical approach to solve transport equations with transport characteristics, changing step-likely with the *e*-folding length, is proposed. It is based on the introduction of a new dependent variable related to the alteration after one time step of the original dependent variable integrated over the volume. Numerical solution of the differential equation for the new variable is found by conjugating exact analytical solutions valid in the vicinity of grid knots. This procedure does not require a priory assumptions on the solution behavior by assessing its derivatives. As an example the formation of transport barriers with heating power exceeding the critical level and under subcritical conditions but with radiation losses dependent nonlinearly on the temperature is simulated.

References

[1] M.G. Worster, Solidification of an alloy from a cooled boundary, J. Fluid Mech. 167 (1986) 481–501.

[2] J. Weiland, Collective Modes in Inhomogeneous Plasma, Institute of Physics Publishing, Bristol, 2000.
[3] ASDEX Team, The H-mode of ASDEX, Nucl. Fusion 29 (1989) 1959–2040.
[4] R.C. Wolf, Internal transport barriers in tokamak plasmas, Plasma Phys. Contr. Fusion 45 (2003) R1–91.
[5] T. Tajima, Computational Plasma Physics, Frontiers in Physics, Westview Press, Boulder, 2004.
[6] H.K. Versteeg, W. Malalasekera, An Introduction to Computational Fluid Dynamics: The Finite Volume Method, Harlow-Longman Scientific & Technical, London, 1995.
[7] A. Clémençon, G. Guivarch, S.P. Eury, X.L. Zou, G. Giruzzi, Analytical solution of the diffusion equation in a cylindrical medium with step-like diffusivity, Phys. Plasmas 11 (2004) 4998–5009.
[8] M.Z. Tokar, A method of numerical solution of ordinary differential equations of second order, Report of Forschungszentrum Jülich, Jül-3208, 1996.
[9] M.Z. Tokar, D. Kalupin, D. Pilipenko, Numerical solution of transport equations for plasmas with transport barrier, Comput. Phys. Commun. 175 (2006) 30–35.
[10] <http://www.efda-itm.eu/>.
[11] L.F. Shampine, Numerical Solution of Ordinary Differential Equations, Chapman and Hall, NY, 1994.
[12] J.I. Ramos, On the numerical treatment of an ordinary differential equation arising in one-dimensional non-Fickian diffusion problems, Comput. Phys. Commun. 170 (2005) 231–238.
[13] M.Z. Tokar, Numerical solution of continuity equation with a flux non-linearly depending on the density gradient, J. Comput. Phys. 220 (2006) 175–183.
[14] M.Z. Tokar, Mechanisms of impurity influence in fusion plasmas, in: S.G. Pandalai (Ed.), Recent Research Developments in Plasmas, vol. 2, Transworld Research Network, Trivandrum, 2002, pp. 99–152.